Finite Volume Methods for Multi-Symplectic PDEs

Sebastian Reich
Department of Mathematics and Statistics
University of Surrey, Guildford, GU2 5XH

January 21, 2000

Abstract

We investigate the application of a cell-vertex finite volume discretization to multi-symplectic PDEs. The investigated discretization reduces to the Preissman box scheme when used on a rectangular grid. Concerning arbitrary quadrilateral grids, we show that only methods with parallelogram-like finite volume cells lead to a multi-symplectic discretization; i.e., to a method that preserves a discrete conservation law of symplecticity.

One of the advantages of finite volume methods is that they can be easily adjusted to variable meshes. But, although the implementation of moving mesh finite volume methods for multi-symplectic PDEs is rather straightforward, the restriction to parallelogram-like cells implies that only meshes moving with a constant speed are multi-symplectic. To overcome this restriction, we suggest the implementation of reversible moving mesh methods based on a semi-Lagrangian approach. Numerical experiments are presented for a one dimensional dispersive shallow-water system.

1 Introduction

Consider the vector-valued first order partial differential equation

$$\partial_\xi \boldsymbol{f}(\boldsymbol{z}) + \partial_\eta \boldsymbol{g}(\boldsymbol{z}) = \boldsymbol{h}(\boldsymbol{z}) \tag{1}$$

in the independent variables $(\xi,\eta) \in \mathbb{R}^2$ and the dependent variable $\boldsymbol{z} \in \mathbb{R}^n$. We say that (1) represents a system of *conservation laws* with *source term* $\boldsymbol{h}(\boldsymbol{z})$. The pair of independent variables (ξ,η) can either stand for two spatial dimensions, in which case we will denote it by (x,y), or for time and one spatial dimension, in which case we will use (x,t). Whenever our considerations are independent of such a differentiation, we will use (ξ,η).

A particular class of PDEs of type (1) is provided by *multi-symplectic* PDEs [2, 3] of the form

$$\mathbf{K}\boldsymbol{z}_\xi + \mathbf{L}\boldsymbol{z}_\eta = \boldsymbol{\nabla}_{\boldsymbol{z}} S(\boldsymbol{z}), \tag{2}$$

where $\boldsymbol{z} \in \mathbb{R}^n$, $S : \mathbb{R}^n \to \mathbb{R}$ some smooth function, and $\mathbf{K}, \mathbf{L}$ are two constant skew-symmetric $n \times n$ matrices.

The *finite volume* method [8, 7] is a popular approach to discretize a PDE of type (1). In particular, when applied to a conservation law

$$\partial_\xi f(\boldsymbol{z}) + \partial_\eta g(\boldsymbol{z}) = 0\,, \tag{3}$$

it leads to a associated discrete conservation law. Any finite volume method applicable to (1) also applies naturally to a multi-symplectic PDE (2). However, (2) is not a collection of conservation laws of type (3). Thus it is not immediately obvious why a finite volume discretization should be preferred over any other discretization approach such as finite differences or pseudo-spectral methods. On the other hand, the special structure of the system (2) implies various "hidden" conservation laws. For example, (2) possesses the associated *conservation law of symplecticity* [2, 3]

$$\partial_\xi \boldsymbol{\kappa} + \partial_\eta \boldsymbol{\lambda} = 0, \tag{4}$$

where

$$\boldsymbol{\kappa} = \boldsymbol{dz} \wedge \mathbf{K}\boldsymbol{dz} \quad \text{and} \quad \boldsymbol{\lambda} = \boldsymbol{dz} \wedge \mathbf{L}\boldsymbol{dz}$$

are pre-symplectic two-forms. This conservation law follows from the *variational equation*

$$\mathbf{K}\boldsymbol{dz}_\xi + \mathbf{L}\boldsymbol{dz}_\eta = S_{\boldsymbol{zz}}(\boldsymbol{z})\boldsymbol{dz} \tag{5}$$

for the vector of one-forms $\boldsymbol{dz} \in L(\mathbb{R}^n, \mathbb{R}^n)$. Upon taking the wedge product of (5) with $\boldsymbol{dz} \in L(\mathbb{R}^n, \mathbb{R}^n)$, we obtain

$$\boldsymbol{dz} \wedge \mathbf{K}\boldsymbol{dz}_\xi + \boldsymbol{dz} \wedge \mathbf{L}\boldsymbol{dz}_\eta = 0,$$

since[1]

$$\boldsymbol{dz} \wedge S_{\boldsymbol{zz}}(\boldsymbol{z})\boldsymbol{dz} = 0$$

as well as

$$\boldsymbol{dz} \wedge \mathbf{L}\boldsymbol{dz}_\eta = \boldsymbol{dz}_\eta \wedge \mathbf{L}\boldsymbol{dz} \quad \text{and} \quad \boldsymbol{dz} \wedge \mathbf{K}\boldsymbol{dz}_\xi = \boldsymbol{dz}_\xi \wedge \mathbf{K}\boldsymbol{dz}.$$

Furthermore, each independent variable gives rise to a *momentum conservation law* of the form [2, 3]

$$\partial_\xi F + \partial_\eta G = 0, \tag{6}$$

with either

$$F(\boldsymbol{z}) = S(\boldsymbol{z}) - \frac{1}{2}\langle \boldsymbol{z}, \mathbf{L}\boldsymbol{z}_\eta \rangle \quad \text{and} \quad G(\boldsymbol{z}) = \frac{1}{2}\langle \boldsymbol{z}, \mathbf{L}\boldsymbol{z}_\xi \rangle, \tag{7}$$

or

$$F(\boldsymbol{z}) = \frac{1}{2}\langle \boldsymbol{z}, \mathbf{K}\boldsymbol{z}_\eta \rangle \quad \text{and} \quad G(\boldsymbol{z}) = S(\boldsymbol{z}) - \frac{1}{2}\langle \boldsymbol{z}, \mathbf{K}\boldsymbol{z}_\xi \rangle, \tag{8}$$

where $\langle \boldsymbol{a}, \boldsymbol{b} \rangle = \boldsymbol{a}^T \boldsymbol{b}$ denotes the Euclidean inner product on $\mathbb{R}^n$. These two conservation laws are obtained by taking the inner product of (2) with either $\boldsymbol{z}_\xi$ or $\boldsymbol{z}_\eta$, respectively. As we will see in the examples below, the partial derivatives in the expressions for F and G can often (but not always) be eliminated. If one of the independent variables is time, then the associated conservation law (6) is called an *energy conservation law* (ECL).

A multi-symplectic PDE (4) might also satisfy a *reversing symmetry*. Following the definition given in [2], we say that (4) satisfies the reversing symmetry $(\mathbf{R}, \mathbf{J})$, if replacing $\boldsymbol{z}$ by $\mathbf{R}\boldsymbol{z}$ and $(\xi, \eta)^T$ by $\mathbf{J}(\xi, \eta)^T$ in (4) leads back to the given PDE (4). Here $\mathbf{R} \in \mathbb{R}^{n \times n}$ and $\mathbf{J} \in \mathbb{R}^{2 \times 2}$ are two *involutions*; i.e., $\mathbf{R} = \mathbf{R}^{-1}$ and $\mathbf{J} = \mathbf{J}^{-1}$, and $\mathbf{J}$ is also diagonal. The existence of a reversing symmetry $(\mathbf{R}, \mathbf{J})$ implies that

$$\bar{\boldsymbol{z}}(\xi, \eta) := \mathbf{R}\boldsymbol{z}(\bar{\xi}, \bar{\eta}), \qquad (\bar{\xi}, \bar{\eta})^T = \mathbf{J}(\xi, \eta)^T,$$

is a solution of (4), if $\boldsymbol{z}(\xi, \eta)$ is a solution of (4). In this paper, we will exclusively deal with the situation that $S(\boldsymbol{z}) = S(\mathbf{R}\boldsymbol{z})$. Hence, $\xi \to \pm\xi$ implies

$$\mathbf{R}^T \mathbf{K} \mathbf{R} = \pm \mathbf{K}$$

and $\eta \to \pm\eta$ implies

$$\mathbf{R}^T \mathbf{L} \mathbf{R} = \pm \mathbf{L}.$$

Let us discuss now the concept of a multi-symplectic PDE by means of two examples.

[1] The wedge product of two differential one forms $\boldsymbol{da}, \boldsymbol{db} \in L(\mathbb{R}^n, \mathbb{R}^n)$ satisfies $\boldsymbol{da} \wedge \boldsymbol{db} = -\boldsymbol{db} \wedge \boldsymbol{da}$. Furthermore, if $\boldsymbol{A}$ is a linear transformation on the linear space $L(\mathbb{R}^n, \mathbb{R}^n)$, then $\boldsymbol{da} \wedge \boldsymbol{A}\boldsymbol{db} = \boldsymbol{A}^T \boldsymbol{da} \wedge \boldsymbol{db}$.

Example 1. Consider the second order elliptic equation

$$u_{xx} + u_{yy} + V(u) = 0, \tag{9}$$

where $V(u)$ is a smooth function. We introduce the state variable $\boldsymbol{z} = (u, v, w)^T$ with $v = u_x$ and $w = u_y$. This yields the system [2]

$$-v_x - w_y = V'(u), \quad u_x = v, \quad u_y = w,$$

which is of the form (2) with

$$S = \frac{v^2 + w^2}{2} + V(u)$$

and the two constant skew-symmetric matrices

$$\mathbf{K} = \begin{bmatrix} 0 & -1 & 0 \\ 1 & 0 & 0 \\ 0 & 0 & 0 \end{bmatrix}, \qquad \mathbf{L} = \begin{bmatrix} 0 & 0 & -1 \\ 0 & 0 & 0 \\ 1 & 0 & 0 \end{bmatrix}.$$

The associated conservation law of symplecticity is

$$\partial_x[\boldsymbol{d}u \wedge \boldsymbol{d}v] + \partial_y[\boldsymbol{d}u \wedge \boldsymbol{d}w] = 0 \tag{10}$$

The two momentum conservation laws (6) are equivalent to

$$\left(\frac{w^2 - v^2}{2} + V(u)\right)_x + (vw)_y = 0 \qquad \text{and} \qquad (vw)_x + \left(\frac{v^2 - w^2}{2} + V(u)\right)_y = 0.$$

There is another "obvious" conservation law $v_y = w_x \ (= u_{xy})$.

It has been shown in [4] that the standard finite difference approximation of the elliptic equation (9); i.e.,

$$-\frac{v_k^{n+1/2} - v_k^{n-1/2}}{\Delta x} - \frac{w_{k+1/2}^n - w_{k-1/2}^n}{\Delta y} = V'(u_k^n), \quad \frac{u_k^{n+1} - u_k^n}{\Delta x} = v_k^{n+1/2}, \quad \frac{u_{k+1}^n - u_k^n}{\Delta y} = w_{k+1/2}^n,$$

leads to a numerical method that exactly conserves a discrete approximation of the conservation law (10); i.e.,

$$\frac{\boldsymbol{d}u_k^{n+1} \wedge \boldsymbol{d}v_k^{n+1/2} - \boldsymbol{d}u_k^n \wedge \boldsymbol{d}v_k^{n-1/2}}{\Delta x} + \frac{\boldsymbol{d}u_{k+1}^n \wedge \boldsymbol{d}v_{k+1/2}^n - \boldsymbol{d}u_k^n \wedge \boldsymbol{d}v_{k-1/2}^n}{\Delta y} = 0.$$

Numerical evidence indicates that this also implies good energy and momentum conservation [16].

The multi-symplectic formulation of (9) satisfies, for example, the reversing symmetry [2]

$$\mathbf{R} = \begin{bmatrix} 1 & 0 & 0 \\ 0 & -1 & 0 \\ 0 & 0 & -1 \end{bmatrix} \quad \text{and} \quad \mathbf{J} = \begin{bmatrix} -1 & 0 \\ 0 & -1 \end{bmatrix},$$

which is maintained under the standard finite difference approximation. ◇

Example 2. Let us now consider the system of conservation laws

$$u_t + \left(\frac{1}{2}u^2 + c_o^2 h\right)_x = 0, \tag{11}$$

$$h_t + (u + hu))_x = 0. \tag{12}$$

These equations are the standard one dimensional shallow-water equations [19]. The variable $u \in \mathbb{R}$ represents the horizontal fluid velocity and $h \in \mathbb{R}$ denotes the deviation of the layer depth $H > 0$ from its mean value $\bar{H} = 1$; i.e., $h = H - 1$. The parameter $c_o > 0$ is the absolute value of the linear phase speed of high-frequency gravity waves. Since the standard shallow-water model exhibits formation of shocks, the dispersive modification

$$\begin{aligned} u_t + \left(\frac{1}{2}u^2 + c_o^2 h + \alpha^2 h_{tt}\right)_x &= 0 \qquad (13)\\ h_t + (u + hu)_x &= 0 \qquad (14)\end{aligned}$$

has been suggested by Boussinesq [19]. Here $\alpha > 0$ is a small parameter.

We reformulate (13)-(14) as a multi-symplectic PDE.[2] Introduce potentials (ϕ, ψ) via $\phi_x := u$, $\psi_x := h$, and two variables (v, w) satisfying

$$v_x = (u + hu)_x \quad \text{and} \quad w_x = \left(\frac{1}{2}u^2 + c_o^2 h + \alpha^2 h_{tt}\right)_x .$$

These definitions, the equations (13)-(14), and $s := \alpha h_t$ yield the system of equations

$$\begin{bmatrix} 0 & 0 & 0 & 0 & 0 & 0 & 0 \\ 0 & 0 & 0 & 0 & 0 & 0 & 0 \\ 0 & 0 & 0 & 0 & 0 & 1 & 0 \\ 0 & 0 & 0 & 0 & 1 & 0 & 0 \\ 0 & 0 & 0 & -1 & 0 & 0 & 0 \\ 0 & 0 & -1 & 0 & 0 & 0 & 0 \\ 0 & 0 & 0 & 0 & 0 & 0 & 0 \end{bmatrix} \begin{pmatrix} u \\ h \\ \phi \\ \psi \\ w \\ v \\ s \end{pmatrix}_x +$$
$$\begin{bmatrix} 0 & 0 & 0 & -1 & 0 & 0 & 0 \\ 0 & 0 & -1 & 0 & 0 & 0 & -2\alpha \\ 0 & 1 & 0 & 0 & 0 & 0 & 0 \\ 1 & 0 & 0 & 0 & 0 & 0 & 0 \\ 0 & 0 & 0 & 0 & 0 & 0 & 0 \\ 0 & 0 & 0 & 0 & 0 & 0 & 0 \\ 0 & 2\alpha & 0 & 0 & 0 & 0 & 0 \end{bmatrix} \begin{pmatrix} u \\ h \\ \phi \\ \psi \\ w \\ v \\ s \end{pmatrix}_t = \begin{pmatrix} 2(u + uh) - v \\ u^2 + 2c_o^2 h - w \\ 0 \\ 0 \\ -h \\ -u \\ 2s \end{pmatrix} . \qquad (15)$$

This system is of the form (2) with state variable $\boldsymbol{z} = (u, h, \phi, \psi, w, v, s)^T \in \mathbb{R}^7$ and Hamiltonian

$$S = (1 + h)u^2 + c_o^2 h^2 + s^2 - vu - wh.$$

Note that the solutions of (15) satisfy

$$(\psi_t + v)_x = 0 \quad \text{and} \quad (\phi_t + w)_x = 0.$$

In fact, one can always choose ψ and ϕ such that $\psi_t = -v$ and $\phi_t = -w$ which we will assume from now on. This assumption also implies that

$$v = u + hu \qquad \text{and} \qquad w = \frac{1}{2}u^2 + c_o^2 h + \alpha^2 h_{tt}.$$

The conservation law of symplecticity (4) is equivalent to

$$\partial_x \left[\boldsymbol{d}\phi \wedge \boldsymbol{d}w + \boldsymbol{d}\psi \wedge \boldsymbol{d}v\right] - \partial_t \left[\boldsymbol{d}u \wedge \boldsymbol{d}\psi + \boldsymbol{d}h \wedge \boldsymbol{d}\phi - 2\alpha \boldsymbol{d}h \wedge \boldsymbol{d}s\right] = 0.$$

[2] A different multi-symplectic formulation of (13)-(14) can be found in [2]. However this formulation is not applicable to the case $\alpha = 0$.

Next we derive the energy conservation law. We first obtain

$$\begin{aligned}\partial_t S &= \phi_t v_x + \psi_t w_x - w_t \psi_x - v_t \phi_x \\ &= (\phi_t v)_x - (v\phi_x)_t + (\psi_t w)_x - (w\psi_x)_t \\ &= -(uv)_t - (wh)_t - 2(wv)_x \,.\end{aligned}$$

Upon using $v = -\psi_t$ and $w = -\phi_t$, this equation is equivalent to the energy conservation law

$$\left((1+h)u^2 + c_o^2 h^2 + s^2\right)_t + 2(wv)_x = 0. \tag{16}$$

One can linearize the system (13)-(14) about its mean layer depth $\bar{H} = 1$ provided $|u| \ll 1$ and $|h| \ll 1$. The corresponding linearized shallow-water equations can be written as

$$\begin{bmatrix} 0 & 0 & 0 & 0 & 0 & 0 & 0 \\ 0 & 0 & 0 & 0 & 0 & 0 & 0 \\ 0 & 0 & 0 & 0 & 0 & 1 & 0 \\ 0 & 0 & 0 & 0 & 1 & 0 & 0 \\ 0 & 0 & 0 & -1 & 0 & 0 & 0 \\ 0 & 0 & -1 & 0 & 0 & 0 & 0 \\ 0 & 0 & 0 & 0 & 0 & 0 & 0 \end{bmatrix} \begin{pmatrix} u \\ h \\ \phi \\ \psi \\ w \\ v \\ s \end{pmatrix}_x +$$
$$\begin{bmatrix} 0 & 0 & 0 & -1 & 0 & 0 & 0 \\ 0 & 0 & -1 & 0 & 0 & 0 & -2\alpha \\ 0 & 1 & 0 & 0 & 0 & 0 & 0 \\ 1 & 0 & 0 & 0 & 0 & 0 & 0 \\ 0 & 0 & 0 & 0 & 0 & 0 & 0 \\ 0 & 0 & 0 & 0 & 0 & 0 & 0 \\ 0 & 2\alpha & 0 & 0 & 0 & 0 & 0 \end{bmatrix} \begin{pmatrix} u \\ h \\ \phi \\ \psi \\ w \\ v \\ s \end{pmatrix}_t = \begin{pmatrix} 2u - v \\ 2c_o^2 h - w \\ 0 \\ 0 \\ -h \\ -u \\ 2s \end{pmatrix}. \tag{17}$$

This system is again of the form (2) with state vector $\boldsymbol{z} = (u, h, \phi, \psi, w, v, s)^T$ and Hamiltonian

$$S = u^2 + c_o^2 h^2 + s^2 - vu - wh.$$

The linearized shallow-water equations possess the energy conservation law

$$\left(u^2 + c_o^2 h^2 + s^2\right)_t + 2(wv)_x = 0. \tag{18}$$

Note that (17) is equivalent to the dispersive linear wave equation

$$u_t + c_o^2 h_x + \alpha^2 h_{xtt} = 0, \qquad h_t + u_x = 0,$$

which reduces to the standard linear wave equation for $\alpha = 0$.

Finally, the system (15) satisfies a reversing symmetry $(\mathbf{R}, \mathbf{J})$ defined by

$$\mathbf{R}\boldsymbol{z} = (u, h, -\phi, -\psi, w, v, -s)^T \quad \text{and} \quad \mathbf{J}(x,t)^T = (-x, -t)^T \,.$$

This symmetry reflects the fact that (13)-(14) are invariant under the involutions $(x,t) \to (-x,-t)$ and $(u,h) \to (u,h)$. There is also a time-reversal symmetry, which is characterized by the involutions $(x,t) \to (x,-t)$ and $(u,h) \to (-u,h)$. Hence

$$\mathbf{R}\boldsymbol{z} = (-u, h, -\phi, \psi, w, -v, -s)^T \quad \text{and} \quad \mathbf{J}(x,t)^T = (x, -t)^T \,.$$

$\diamond$

Discretization methods for (2) that preserve a discrete conservation law of symplecticity have been discussed in [4, 16]. We call such methods *multi-symplectic integrators* [13]. While the multi-symplectic methods in [4, 16] are based on the general idea of *Runge-Kutta collocation methods*, multi-symplectic methods based on a *discrete Lagrangian formulation* have been discussed in [13]. It has been demonstrated in [16] that multi-symplectic methods exhibit excellent energy-momentum conservation properties.

The aim of this paper is twofold. (i) We like to investigate finite volume discretizations of (2) and wish to establish conditions under which such a discretization implies a corresponding finite volume discretization of the "hidden" conservation laws (4) and (6). We will focus on a particular *cell-vertex method* [15, 8] which is described in §2. In §3-4, we will derive conditions on the grid structure that implies discrete conservation of symplecticity and momentum. We stress that we only consider smooth solutions of (2) and do not discuss the computation of shocks.

(ii) Even when computing smooth solutions of time-dependent problems, it might be desirable to adjust the mesh in an appropriate way. One popular choice to do so it to implement a *moving mesh method* (see, for example, [9, 10, 6, 5, 12] and references therein). One advantage of the finite volume approach considered here is that it allows for a rather straightforward implementation of moving meshes. However, while general moving mesh finite volume methods cannot be expected to preserve the conservation laws of symplecticity and momentum exactly, a moving mesh strategy may nevertheless respect a reversing symmetry of the given system. This is discussed in §6 where a *reversible moving mesh method* is proposed. In §7, numerical results are presented for the dispersive shallow-water system (13)-(14).

The finite volume discretization, as considered in this paper for time-dependent problems, can be viewed as complementary to the finite volume method introduced in [11] for hyperbolic PDEs. Our method is also a natural generalization of the *Preissman box scheme* [1, 4] to arbitrary mesh configurations (see [14] for details in the context of convection dominated diffusion equations).

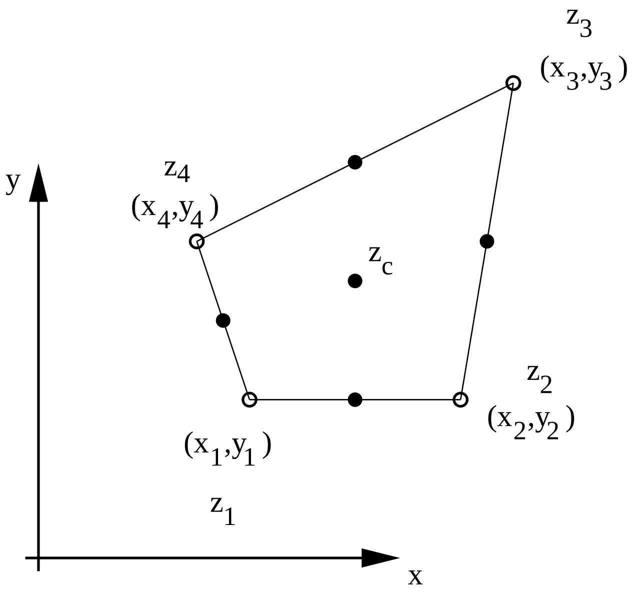

Figure 1: A finite volume cell, with cell-vertex ∘, the edge center •, and the cell center • points.

2 A Cell-Vertex Method

We shall now consider a structured mesh which is topologically equivalent to a rectangular mesh. The integral of (1) over a quadrilateral finite volume (or cell) is given by

$$\frac{1}{V_C}\int_{\Omega_C}\left(\partial_\xi \boldsymbol{f}(\boldsymbol{z})+\partial_\eta \boldsymbol{g}(\boldsymbol{z})\right)\,d\xi d\eta=\frac{1}{V_C}\int_{\Omega_C}\boldsymbol{h}(\boldsymbol{z})\,d\xi d\eta$$

which is equivalent to

$$\frac{1}{V_C}\oint_{\partial\Omega_C}\left(\boldsymbol{f}(\boldsymbol{z})\,d\eta-\boldsymbol{g}(\boldsymbol{z})\,d\xi\right)=\frac{1}{V_C}\int_{\Omega_C}\boldsymbol{h}(\boldsymbol{z})\,d\xi d\eta, \tag{19}$$

where V_C is the oriented area (volume) of the cell.

We now use the cell-vertex approach [15, 8] to discretize this equation. The unknowns $\boldsymbol{z}_i$ are held at the cell vertices (ξ_i,η_i), $i=1,\ldots,4$. See Fig. 1, where the independent variables are denoted by (x,y). The *midpoint/trapezoidal rule* is used along the edges to calculate the fluxes.[3] To do so we introduce the midpoint/trapezoidal approximations

$$\boldsymbol{z}_{ij}=\frac{\boldsymbol{z}_i+\boldsymbol{z}_j}{2},$$

$i,j=1,\ldots,4$. Thus (19) is replaced by the discretized equation

$$\begin{aligned}\frac{1}{V_C}\left(\boldsymbol{f}(\boldsymbol{z}_{12})(\eta_2-\eta_1)+\boldsymbol{f}(\boldsymbol{z}_{23})(\eta_3-\eta_2)+\boldsymbol{f}(\boldsymbol{z}_{34})(\eta_4-\eta_3)+\boldsymbol{f}(\boldsymbol{z}_{41})(\eta_1-\eta_4)\right)-&\\ \frac{1}{V_C}\left(\boldsymbol{g}(\boldsymbol{z}_{12})(\xi_2-\xi_1)+\boldsymbol{g}(\boldsymbol{z}_{23})(\xi_3-\xi_2)+\boldsymbol{g}(\boldsymbol{z}_{34})(\xi_4-\xi_3)+\boldsymbol{g}(\boldsymbol{z}_{41})(\xi_1-\xi_4)\right) &= \boldsymbol{h}_c,\end{aligned} \tag{20}$$

where

$$V_C=-\frac{1}{2}\left[(\xi_2-\xi_4)(\eta_1-\eta_3)+(\xi_3-\xi_1)(\eta_2-\eta_4)\right].$$

This system still requires the definition of

$$\boldsymbol{h}_c\approx\frac{1}{V_C}\int_{\Omega_C}\boldsymbol{h}(\boldsymbol{z})\,d\xi d\eta.$$

In this paper, we will focus on

$$\boldsymbol{h}_c:=\boldsymbol{h}(\boldsymbol{z}_c)\,,\qquad \boldsymbol{z}_c=\frac{\boldsymbol{z}_1+\boldsymbol{z}_2+\boldsymbol{z}_3+\boldsymbol{z}_4}{4}. \tag{21}$$

Another option is provided, for example, by

$$\boldsymbol{h}_c:=\frac{\boldsymbol{h}(\boldsymbol{z}_1)+\boldsymbol{h}(\boldsymbol{z}_2)+\boldsymbol{h}(\boldsymbol{z}_3)+\boldsymbol{h}(\boldsymbol{z}_4)}{4}.$$

This general approach can now also be applied to the multi-symplectic formulation (2). In particular, the integral of (2) over a quadrilateral finite volume (or cell) is given by

$$\frac{1}{V_C}\int_{\Omega_C}\left(\mathbf{K}\boldsymbol{z}_\xi+\mathbf{L}\boldsymbol{z}_\eta\right)\,d\xi d\eta=\frac{1}{V_C}\int_{\Omega_C}\boldsymbol{\nabla}_{\boldsymbol{z}}S(\boldsymbol{z})\,d\xi d\eta$$

[3]Note that, because of the semi-linear form of (2), both the midpoint and the trapezoidal approximation of the fluxes give the same result. However, when evaluating the discrete momentum conservation laws and the discrete conservation law of symplecticity, it is crucial that the midpoint rule is applied.

which is equivalent to

$$\frac{1}{V_C}\oint_{\partial\Omega_C}(\mathbf{K}\boldsymbol{z}\,d\eta - \mathbf{L}\boldsymbol{z}\,d\xi) = \frac{1}{V_C}\int_{\Omega_C}\boldsymbol{\nabla}_{\boldsymbol{z}}S(\boldsymbol{z})\,d\xi d\eta\,.$$

Adapting the discretization (20) to this equation and using (21) to approximate the integral over the source term $\boldsymbol{\nabla}_{\boldsymbol{z}}S(\boldsymbol{z})$, we obtain the approximation

$$\begin{aligned}
&\frac{1}{V_C}\mathbf{K}\left(\frac{\boldsymbol{z}_1+\boldsymbol{z}_2}{2}(\eta_2-\eta_1)+\frac{\boldsymbol{z}_2+\boldsymbol{z}_3}{2}(\eta_3-\eta_2)+\frac{\boldsymbol{z}_3+\boldsymbol{z}_4}{2}(\eta_4-\eta_3)+\frac{\boldsymbol{z}_4+\boldsymbol{z}_1}{2}(\eta_1-\eta_4)\right)- \\
&\quad\frac{1}{V_C}\mathbf{L}\left(\frac{\boldsymbol{z}_1+\boldsymbol{z}_2}{2}(\xi_2-\xi_1)+\frac{\boldsymbol{z}_2+\boldsymbol{z}_3}{2}(\xi_3-\xi_2)+\frac{\boldsymbol{z}_3+\boldsymbol{z}_4}{2}(\xi_4-\xi_3)+\frac{\boldsymbol{z}_4+\boldsymbol{z}_1}{2}(\xi_1-\xi_4)\right) \\
&\qquad = \boldsymbol{\nabla}_{\boldsymbol{z}}S(\boldsymbol{z}_c),
\end{aligned}\tag{22}$$

which is equivalent to

$$\begin{aligned}
&\frac{1}{2V_C}\left[(\mathbf{K}\boldsymbol{z}_1-\mathbf{K}\boldsymbol{z}_3)(\eta_2-\eta_4)+(\mathbf{K}\boldsymbol{z}_2-\mathbf{K}\boldsymbol{z}_4)(\eta_3-\eta_1)\right]- \\
&\quad\frac{1}{2V_C}\left[(\mathbf{L}\boldsymbol{z}_1-\mathbf{L}\boldsymbol{z}_3)(\xi_2-\xi_4)+(\mathbf{L}\boldsymbol{z}_2-\mathbf{L}\boldsymbol{z}_4)(\xi_3-\xi_1)\right] \quad = \quad \boldsymbol{\nabla}_{\boldsymbol{z}}S(\boldsymbol{z}_c).
\end{aligned}$$

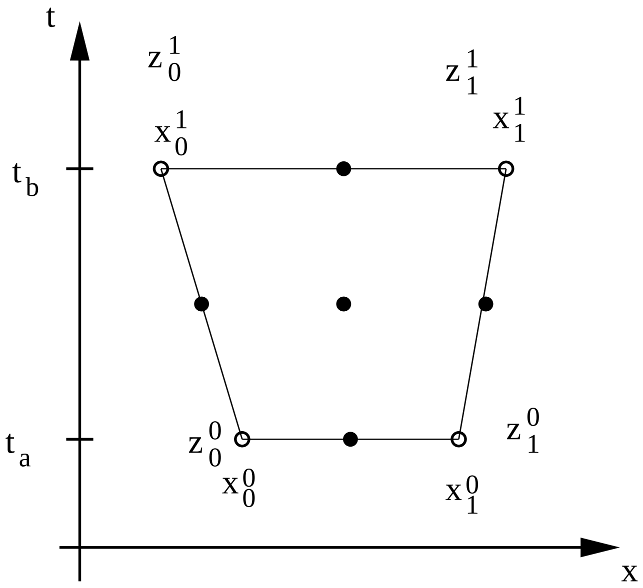

Figure 2: A finite volume cell (trapezoid) in time t and space x, with cell-vertex $\circ$, the edge center $\bullet$, and the cell centre $\bullet$ points.

This scheme can, in principle, be applied to systems where (ξ,η) represent two spatial directions or to systems where η represents time. However, for systems with $(\xi,\eta)=(x,t)$, one typically imposes the restriction that the discretization is "flat" in the temporal direction. To be more specific, let us consider the system

$$\mathbf{K}\boldsymbol{z}_x+\mathbf{L}\boldsymbol{z}_t=\boldsymbol{\nabla}_{\boldsymbol{z}}S(\boldsymbol{z})\,.\tag{23}$$

The corresponding finite volume discretization is obtained by discretizing

$$\frac{1}{V_C}\oint_{\partial\Omega_C}(\mathbf{K}\boldsymbol{z}\,dt-\mathbf{L}\boldsymbol{z}\,dx)=\boldsymbol{\nabla}_{\boldsymbol{z}}S(\boldsymbol{z}_c)\,.$$

We apply the finite volume method (22) with ξ replaced by x and η by t. However, we now impose the restrictions

$$t_a = t_1 = t_2 \quad \text{and} \quad t_b = t_3 = t_4. \tag{24}$$

Furthermore, we introduce the independent variables $(x_0^0, x_1^0, x_1^1, x_0^1)$ instead of (x_1, x_2, x_3, x_4) and the dependent variables $(\boldsymbol{z}_0^0, \boldsymbol{z}_1^0, \boldsymbol{z}_1^1, \boldsymbol{z}_0^1)$ instead of $(\boldsymbol{z}_1, \boldsymbol{z}_2, \boldsymbol{z}_3, \boldsymbol{z}_4)$. See Fig. 2. Thus we obtain

$$\begin{aligned} &\frac{1}{V_C}\mathbf{K}\left(\frac{\boldsymbol{z}_1^1 + \boldsymbol{z}_1^0}{2}\Delta t - \frac{\boldsymbol{z}_0^0 + \boldsymbol{z}_0^1}{2}\Delta t\right) - \\ \frac{1}{V_C}\mathbf{L}\left(\frac{\boldsymbol{z}_1^1 + \boldsymbol{z}_0^1}{2}(x_0^1 - x_1^1) + \frac{\boldsymbol{z}_1^1 + \boldsymbol{z}_1^0}{2}(x_1^1 - x_1^0) + \frac{\boldsymbol{z}_1^0 + \boldsymbol{z}_0^0}{2}(x_1^0 - x_0^0) + \frac{\boldsymbol{z}_0^0 + \boldsymbol{z}_0^1}{2}(x_0^0 - x_0^1)\right) &\\ = \nabla_{\boldsymbol{z}} S(\boldsymbol{z}_c), \end{aligned} \tag{25}$$

where $\Delta t = t_b - t_a$ and

$$V_C = \Delta t \frac{x_{i+1}^1 + x_{i+1}^0 - x_i^1 - x_i^0}{2}.$$

This discretization is equivalent to the more compact scheme

$$\frac{1}{V_C}\mathbf{K}\left(\frac{\boldsymbol{z}_1^1 + \boldsymbol{z}_1^0}{2}\Delta t - \frac{\boldsymbol{z}_0^0 + \boldsymbol{z}_0^1}{2}\Delta t\right) + \frac{1}{V_C}\mathbf{L}\left(\frac{\boldsymbol{z}_0^1 - \boldsymbol{z}_1^0}{2}(x_1^1 - x_0^0) + \frac{\boldsymbol{z}_1^1 - \boldsymbol{z}_0^0}{2}(x_1^0 - x_0^1)\right) = \nabla_{\boldsymbol{z}} S(\boldsymbol{z}_c).$$

If we also impose the conditions

$$x_a = x_0^0 = x_0^1 \quad \text{and} \quad x_b = x_1^0 = x_1^1,$$

which leads to a rectangular grid, then the *Preissman box scheme* [1, 4]

$$\frac{1}{V_C}\mathbf{K}\left(\frac{\boldsymbol{z}_1^1 + \boldsymbol{z}_1^0}{2}\Delta t - \frac{\boldsymbol{z}_0^0 + \boldsymbol{z}_0^1}{2}\Delta t\right) + \frac{1}{V_C}\mathbf{L}\left(\frac{\boldsymbol{z}_1^1 + \boldsymbol{z}_0^1}{2}\Delta x - \frac{\boldsymbol{z}_1^0 + \boldsymbol{z}_0^0}{2}\Delta x\right) = \nabla_{\boldsymbol{z}} S(\boldsymbol{z}_c),$$

$\Delta x = x_b - x_a$, $V_C = \Delta x \Delta t$, is obtained. The formulation (25) has the conceptual advantage that it allows to implement moving mesh methods in a rather straightforward way. We will discuss this issue in more detail in §6.

One can certainly go to discretization that are not "flat" in time and, therefore, do not obey (24). Instead we introduce $t_1 = t_0^0$, $t_2 = t_1^0$, $t_3 = t_1^1$, and $t_4 = t_0^1$ and obtain the finite volume discretization

$$\begin{aligned} &\frac{1}{2V_C}\left[(\mathbf{K}\boldsymbol{z}_0^0 - \mathbf{K}\boldsymbol{z}_1^1)(t_1^0 - t_0^1) + (\mathbf{K}\boldsymbol{z}_1^0 - \mathbf{K}\boldsymbol{z}_0^1)(t_1^1 - t_0^0)\right] - \\ &\quad \frac{1}{2V_C}\left[(\mathbf{L}\boldsymbol{z}_0^0 - \mathbf{L}\boldsymbol{z}_1^1)(x_1^0 - x_0^1) + (\mathbf{L}\boldsymbol{z}_1^0 - \mathbf{L}\boldsymbol{z}_0^1)(x_1^1 - x_0^0)\right] \quad = \quad \nabla_{\boldsymbol{z}} S(\boldsymbol{z}_c). \end{aligned} \tag{26}$$

This scheme allows one to adjust the method locally in time and space. But we will not investigate this option any further in this paper.

3 The Discrete Multi-Symplectic Conservation Law

We now formally apply a finite volume approximation to the multi-symplectic conservation law (4). We start with the integral formulation

$$\frac{1}{V_C}\int_{\Omega_C} (\partial_\xi \boldsymbol{\kappa} + \partial_\eta \boldsymbol{\lambda})\, d\xi d\eta = 0$$

which is equivalent to

$$\frac{1}{V_C}\oint_{\partial\Omega_C} (\boldsymbol{\kappa}\, d\eta - \boldsymbol{\lambda}\, d\xi) = 0.$$

Next we apply the cell-vertex method (20) which requires the approximation of the two-forms $\boldsymbol{\kappa}$ and $\boldsymbol{\lambda}$ at the center of the edges. We use again the implicit midpoint approximation and obtain, for example, for the 1–2 edge

$$\boldsymbol{\kappa}_{12} = \frac{\boldsymbol{dz}_1 + \boldsymbol{dz}_2}{2} \wedge \mathbf{K}\frac{\boldsymbol{dz}_1 + \boldsymbol{dz}_2}{2}$$

as well as

$$\boldsymbol{\lambda}_{12} = \frac{\boldsymbol{dz}_1 + \boldsymbol{dz}_2}{2} \wedge \mathbf{L}\frac{\boldsymbol{dz}_1 + \boldsymbol{dz}_2}{2}.$$

Thus, in complete analogy to (20), we formally derive the discrete conservation law

$$\begin{aligned}
&\frac{1}{V_C}\left(\boldsymbol{\kappa}_{12}(\eta_2-\eta_1) + \boldsymbol{\kappa}_{23}(\eta_3-\eta_2) + \boldsymbol{\kappa}_{34}(\eta_4-\eta_3) + \boldsymbol{\kappa}_{14}(\eta_1-\eta_4)\right) - \\
&\quad \frac{1}{V_C}\left(\boldsymbol{\lambda}_{12}(\xi_2-\xi_1) + \boldsymbol{\lambda}_{23}(\xi_3-\xi_2) + \boldsymbol{\lambda}_{34}(\xi_4-\xi_3) + \boldsymbol{\lambda}_{14}(\xi_1-\xi_4)\right) \quad = \quad 0,
\end{aligned} \tag{27}$$

where

$$\boldsymbol{\kappa}_{ij} = \frac{\boldsymbol{dz}_i + \boldsymbol{dz}_j}{2} \wedge \mathbf{K}\frac{\boldsymbol{dz}_i + \boldsymbol{dz}_j}{2} \quad \text{and} \quad \boldsymbol{\lambda}_{ij} = \frac{\boldsymbol{dz}_i + \boldsymbol{dz}_j}{2} \wedge \mathbf{L}\frac{\boldsymbol{dz}_i + \boldsymbol{dz}_j}{2}.$$

To shorten the subsequent expressions, we introduce the notation

$$\boldsymbol{dz}_{ij} = \frac{\boldsymbol{dz}_i + \boldsymbol{dz}_j}{2}, \qquad i,j = 1,\ldots,4.$$

The equation (27) requires the definition of the cell-vertex values of the differential $\boldsymbol{dz}$. The natural definition is given by the linearization of our discretization (22); i.e., by the *discrete variational equation*

$$\begin{aligned}
&\frac{1}{V_C}\mathbf{K}\left[\boldsymbol{dz}_{12}(\eta_2-\eta_1) + \boldsymbol{dz}_{23}(\eta_3-\eta_2) + \boldsymbol{dz}_{34}(\eta_4-\eta_3) + \boldsymbol{dz}_{41}(\eta_1-\eta_4)\right] - \\
&\quad \frac{1}{V_C}\mathbf{L}\left[\boldsymbol{dz}_{12}(\xi_2-\xi_1) + \boldsymbol{dz}_{23}(\xi_3-\xi_2) + \boldsymbol{dz}_{34}(\xi_4-\xi_3) + \boldsymbol{dz}_{41}(\xi_1-\xi_4)\right] \\
&\qquad = \quad S_{\boldsymbol{zz}}(\boldsymbol{z}_c)\boldsymbol{dz}_c,
\end{aligned} \tag{28}$$

where

$$\boldsymbol{dz}_c = \frac{1}{4}\left(\boldsymbol{dz}_1 + \boldsymbol{dz}_2 + \boldsymbol{dz}_3 + \boldsymbol{dz}_4\right).$$

We now investigate under which conditions this equation implies the discrete conservation law (27). To find out, we take the wedge product of (28) with $2\boldsymbol{dz}_c$ and obtain

$$\begin{aligned}
&\frac{1}{V_C}\left[\boldsymbol{\kappa}_{12}(\eta_2-\eta_1) + \boldsymbol{\kappa}_{23}(\eta_3-\eta_2) + \boldsymbol{\kappa}_{34}(\eta_4-\eta_3) + \boldsymbol{\kappa}_{14}(\eta_1-\eta_4)\right] - \\
&\frac{1}{V_C}\left[\boldsymbol{\lambda}_{12}(\xi_2-\xi_1) + \boldsymbol{\lambda}_{23}(\xi_3-\xi_2) + \boldsymbol{\lambda}_{34}(\xi_4-\xi_3) + \boldsymbol{\lambda}_{14}(\xi_1-\xi_4)\right] - \\
&\frac{1}{V_C}\left[\boldsymbol{dz}_{12} \wedge \mathbf{K}\boldsymbol{dz}_{34}(\eta_2-\eta_1-\eta_4+\eta_3) - \boldsymbol{dz}_{41} \wedge \mathbf{K}\boldsymbol{dz}_{23}(\eta_2-\eta_3+\eta_1-\eta_4)\right] + \\
&\frac{1}{V_C}\left[\boldsymbol{dz}_{12} \wedge \mathbf{L}\boldsymbol{dz}_{34}(\xi_2-\xi_1-\xi_4+\xi_3) - \boldsymbol{dz}_{41} \wedge \mathbf{L}\boldsymbol{dz}_{23}(\xi_2-\xi_3+\xi_1-\xi_4)\right] \quad = \quad 0,
\end{aligned}$$

where we used that

$$\boldsymbol{dz}_c \wedge S_{\boldsymbol{zz}}(\boldsymbol{z}_c)\boldsymbol{dz}_c = 0.$$

Proposition 1. The discrete conservation law (27) is naturally satisfied by the numerical method (22), if the coordinates (ξ_i, η_i) of the cell vertices satisfy

$$(\eta_2 - \eta_1) + (\eta_3 - \eta_4) = 0 \quad \text{and} \quad (\eta_2 - \eta_3) + (\eta_1 - \eta_4) = 0\,. \tag{29}$$

as well as

$$(\xi_2 - \xi_1) + (\xi_3 - \xi_4) = 0 \quad \text{and} \quad (\xi_2 - \xi_3) + (\xi_1 - \xi_4) = 0. \tag{30}$$

These four conditions are satisfied by cells which take the shape of a *parallelogram*.[4] ⋄

It is interesting to note that it was found in [18] that the cell-vertex finite volume method is second order convergent provided the cells are close to parallelograms in the sense that the distance between the midpoints of the diagonals is $\mathcal{O}(h^2)$ where h is the diameter of the cell.

Assuming that the conditions (29)-(30) hold, we can introduce new variables

$$\Delta\eta_{ew} = \eta_2 - \eta_1, \quad \Delta\eta_{ns} = \eta_3 - \eta_2, \quad \Delta\xi_{ew} = \xi_2 - \xi_1, \quad \Delta\xi_{ns} = \xi_3 - \xi_2.$$

Thus, under the conditions (29)-(30), we can rewrite (22) as

$$\begin{aligned} &\frac{1}{V_C}\mathbf{K}\left(\frac{\boldsymbol{z}_1 + \boldsymbol{z}_2 - \boldsymbol{z}_3 - \boldsymbol{z}_4}{2}\Delta\eta_{ew} + \frac{\boldsymbol{z}_2 + \boldsymbol{z}_3 - \boldsymbol{z}_1 - \boldsymbol{z}_4}{2}\Delta\eta_{ns}\right) - \\ &\quad \frac{1}{V_C}\mathbf{L}\left(\frac{\boldsymbol{z}_1 + \boldsymbol{z}_2 - \boldsymbol{z}_3 - \boldsymbol{z}_4}{2}\Delta\xi_{ew} + \frac{\boldsymbol{z}_2 + \boldsymbol{z}_3 - \boldsymbol{z}_1 - \boldsymbol{z}_4}{2}\Delta\xi_{ns}\right) \quad = \quad \boldsymbol{\nabla}_{\boldsymbol{z}} S(\boldsymbol{z}_c) \end{aligned} \tag{31}$$

and the (oriented) cell volume is simply given by

$$V_C = \Delta\eta_{ns}\Delta\xi_{ew} - \Delta\eta_{ew}\Delta\xi_{ns}.$$

Note that the Preissman box scheme [1] is obtained for $\Delta\eta_{ew} = 0$ and $\Delta\xi_{ns} = 0$. This scheme was shown to be multi-symplectic in [4].

Let us discuss the implications of (29)-(30) on the discretization (25) of a time-dependent PDE (23). Using the above notations, we can write

$$\Delta\eta_{ns} = \Delta t, \quad \Delta\eta_{ew} = 0, \quad \Delta\xi_{ns} = c\Delta t, \quad \Delta\xi_{ew} = \Delta x$$

where Δt is the height of the parallelogram and Δx its width. The constant c represents the skewness of the parallelogram. Thus, when discretizing (23) with a method of type (31) and using a parallelogram-like cell, the resulting scheme is equivalent to applying the Preissman box scheme with time step Δt and mesh size Δx to the "moving frame" PDE

$$(\mathbf{K} - c\mathbf{L})\boldsymbol{z}_x + \mathbf{L}\frac{d}{dt}\boldsymbol{z} = \boldsymbol{\nabla}_{\boldsymbol{z}} S(\boldsymbol{z}), \qquad \frac{d}{dt}x = c. \tag{32}$$

This formulation is of particular interest when computing soliton solutions traveling with a constant wave speed c. Then $d\boldsymbol{z}/dt = \mathbf{0}$ in (32) and one only has to solve a stationary problem.

4 The Discrete Momentum Conservation Laws

The momentum conservation law (6) can be rewritten in integral form as

$$\frac{1}{V_C}\oint_{\partial\Omega_C} (F\,d\eta - G\,d\xi) = 0\,,$$

[4]To be more precise, the grid has to be composed of identical parallelogram-like cells for the method to be multi-symplectic on the whole grid.

where, in the sequel, we focus on the expressions (7) for F and G.

Before applying the finite volume method (20), we have to introduce approximations to the fluxes at the edge centers. We use the midpoint rule and obtain, for example, for the 1–2 edge the formulas

$$\begin{aligned} F_{12} &= S\left(\frac{\boldsymbol{z}_1+\boldsymbol{z}_2}{2}\right) - \frac{1}{2}\langle \frac{\boldsymbol{z}_1+\boldsymbol{z}_2}{2}, \mathbf{L}\frac{(\eta_2-\eta_1)(\boldsymbol{z}_2-\boldsymbol{z}_1)}{(\xi_2-\xi_1)^2+(\eta_2-\eta_1)^2}\rangle \\ &= S\left(\frac{\boldsymbol{z}_1+\boldsymbol{z}_2}{2}\right) - \frac{\eta_2-\eta_1}{2(\eta_2-\eta_1)^2+2(\xi_2-\xi_1)^2}\langle \boldsymbol{z}_1, \mathbf{L}\boldsymbol{z}_2\rangle \end{aligned}$$

and

$$G_{12} = \frac{\xi_2-\xi_1}{2(\xi_2-\xi_1)^2+2(\eta_2-\eta_1)^2}\langle \boldsymbol{z}_1, \mathbf{L}\boldsymbol{z}_2\rangle.$$

Upon deriving similar expressions for the other three edges, we derive the discrete momentum conservation law

$$\begin{aligned} &\frac{1}{V_C}\left[F_{12}(\eta_2-\eta_1)+F_{23}(\eta_3-\eta_2)+F_{34}(\eta_4-\eta_3)+F_{41}(\eta_1-\eta_4)\right] - \\ &\quad \frac{1}{V_C}\left[G_{12}(\xi_2-\xi_1)+G_{23}(\xi_3-\xi_2)+G_{34}(\xi_4-\xi_3)+G_{41}(\xi_1-\xi_4)\right] = 0 \end{aligned}$$

from the general formula (20). Note that, for example,

$$F_{12}(\eta_2-\eta_1) - G_{12}(\xi_2-\xi_1) = S\left(\frac{\boldsymbol{z}_1+\boldsymbol{z}_2}{2}\right)(\eta_2-\eta_1) - \frac{1}{2}\langle \boldsymbol{z}_1, \mathbf{L}\boldsymbol{z}_2\rangle.$$

This allows us to obtain the more compact formulation

$$\begin{aligned} &\left(S(\boldsymbol{z}_{12})(\eta_2-\eta_1)+S(\boldsymbol{z}_{23})(\eta_3-\eta_2)+S(\boldsymbol{z}_{34})(\eta_4-\eta_3)+S(\boldsymbol{z}_{41})(\eta_1-\eta_4)\right) - \\ &\quad \left(\langle \boldsymbol{z}_1, \mathbf{L}\boldsymbol{z}_2\rangle + \langle \boldsymbol{z}_2, \mathbf{L}\boldsymbol{z}_3\rangle + \langle \boldsymbol{z}_3, \mathbf{L}\boldsymbol{z}_4\rangle + \langle \boldsymbol{z}_4, \mathbf{L}\boldsymbol{z}_1\rangle\right) = 0. \end{aligned} \tag{33}$$

Provided that the conditions (29)-(30) hold, equation (33 is equivalent to

$$\begin{aligned} &\left[S(\boldsymbol{z}_{12}) - S(\boldsymbol{z}_{34})\right]\Delta\eta_{ew} + \left[S(\boldsymbol{z}_{23}) - S(\boldsymbol{z}_{41})\right]\Delta\eta_{ns} - \\ &\quad \left(\langle \boldsymbol{z}_1, \mathbf{L}\boldsymbol{z}_2\rangle + \langle \boldsymbol{z}_2, \mathbf{L}\boldsymbol{z}_3\rangle + \langle \boldsymbol{z}_3, \mathbf{L}\boldsymbol{z}_4\rangle + \langle \boldsymbol{z}_4, \mathbf{L}\boldsymbol{z}_1\rangle\right) = 0. \end{aligned} \tag{34}$$

We show now that for linear PDEs of type (2); i.e.

$$S(\boldsymbol{z}) = \frac{1}{2}\langle \boldsymbol{z}, \mathbf{A}\boldsymbol{z}\rangle,$$

$\mathbf{A}$ a symmetric $n \times n$ matrix, the cell-vertex method (22) implies (34) automatically provided the conditions (29)-(30) hold. To do so we take the inner product of (31) with

$$\boldsymbol{a} := \frac{\boldsymbol{z}_1+\boldsymbol{z}_2-\boldsymbol{z}_3-\boldsymbol{z}_4}{2}\Delta\eta_{ew} + \frac{\boldsymbol{z}_2+\boldsymbol{z}_3-\boldsymbol{z}_1-\boldsymbol{z}_4}{2}\Delta\eta_{ns}\,.$$

This yields

$$\begin{aligned} \langle \boldsymbol{a}, \boldsymbol{A}\boldsymbol{z}_c\rangle &= \langle \frac{\boldsymbol{z}_1+\boldsymbol{z}_2}{2}, \boldsymbol{A}\frac{\boldsymbol{z}_1+\boldsymbol{z}_2}{4}\rangle\Delta\eta_{ew} - \langle \frac{\boldsymbol{z}_3+\boldsymbol{z}_4}{2}, \boldsymbol{A}\frac{\boldsymbol{z}_3+\boldsymbol{z}_4}{4}\rangle\Delta\eta_{ew} - \\ &\quad \langle \frac{\boldsymbol{z}_1+\boldsymbol{z}_4}{2}, \boldsymbol{A}\frac{\boldsymbol{z}_1+\boldsymbol{z}_4}{4}\rangle\Delta\eta_{ns} + \langle \frac{\boldsymbol{z}_2+\boldsymbol{z}_3}{2}, \boldsymbol{A}\frac{\boldsymbol{z}_2+\boldsymbol{z}_3}{4}\rangle\Delta\eta_{ns} \\ &= \left[S\left(\frac{\boldsymbol{z}_1+\boldsymbol{z}_2}{2}\right) - S\left(\frac{\boldsymbol{z}_3+\boldsymbol{z}_4}{2}\right)\right]\Delta\eta_{ew} + \left[S\left(\frac{\boldsymbol{z}_2+\boldsymbol{z}_3}{2}\right) - S\left(\frac{\boldsymbol{z}_4+\boldsymbol{z}_1}{2}\right)\right]\Delta\eta_{ns} \end{aligned}$$

and

$$\begin{aligned}\frac{1}{V_C}\langle \boldsymbol{a}, \mathbf{L}\boldsymbol{b}\rangle &= \frac{1}{4}\langle(\boldsymbol{z}_1+\boldsymbol{z}_2-\boldsymbol{z}_3+\boldsymbol{z}_4), \mathbf{L}(\boldsymbol{z}_2+\boldsymbol{z}_3-\boldsymbol{z}_1-\boldsymbol{z}_4)\rangle \\ &= \frac{1}{2}\left[\langle \boldsymbol{z}_1, \mathbf{L}\boldsymbol{z}_2\rangle + \langle \boldsymbol{z}_2, \mathbf{L}\boldsymbol{z}_3\rangle + \langle \boldsymbol{z}_3, \mathbf{L}\boldsymbol{z}_4\rangle + \langle \boldsymbol{z}_4, \mathbf{L}\boldsymbol{z}_1\rangle\right],\end{aligned}$$

where

$$\boldsymbol{b} := \frac{\boldsymbol{z}_1+\boldsymbol{z}_2-\boldsymbol{z}_3-\boldsymbol{z}_4}{2}\Delta\xi_{ew} + \frac{\boldsymbol{z}_2+\boldsymbol{z}_3-\boldsymbol{z}_1-\boldsymbol{z}_4}{2}\Delta\xi_{ns}.$$

Since also

$$\frac{1}{V_C}\langle \boldsymbol{a}, \mathbf{K}\boldsymbol{a}\rangle = 0,$$

the desired result follows.

A corresponding result holds for the conservation law (6) with F and G defined by (8).

Proposition 2. Let us consider a linear PDE (2); i.e.,

$$S(\boldsymbol{z}) = \frac{1}{2}\langle \boldsymbol{z}, \boldsymbol{A}\boldsymbol{z}\rangle,$$

and discretize the system by a finite volume discretization (22). Then the numerical approximations exactly satisfy the discrete momentum conservation law (34), if the conditions (29)-(30) hold (parallelogram-like cell structure). $\diamond$

5 Discretization of the Dispersive Shallow-Water Equations

Let us apply the discretization (25) to the multi-symplectic formulation (15) of the dispersive shallow-water equations (13)-(14). We describe this discretization in more detail for the case of periodic boundary conditions. Thus, instead of looking at one finite volume cell, we consider M cells with grid points $\{x_i^0\}$ at $t=0$ and grid points $\{x_i^1\}$ at time $t=\Delta t$. Let $\boldsymbol{I}\in\mathbb{R}^{M\times M}$ denote the identity matrix and $\boldsymbol{E}=\{e_{ij}\}\in\mathbb{R}^{M\times M}$ the shift matrix defined by

$$e_{ij} = \begin{cases} 1 & j = i+1 \ (\mathrm{mod}\, M) \\ 0 & j \neq i \ (\mathrm{mod}\, M) \end{cases}$$

We also introduce the averaging operator

$$\boldsymbol{A} = \frac{1}{2}(\boldsymbol{I}+\boldsymbol{E})$$

and the differencing operator

$$\boldsymbol{D} = \boldsymbol{E} - \boldsymbol{I}.$$

The variables $(\{u_i^n\},\{h_i^n\},\{v_i^n\},\{w_i^n\},\{\phi_i^n\},\{\psi_i^n\},\{s_i^n\})$ are collected in the vectors $(\boldsymbol{u}^n,\boldsymbol{h}^n,\boldsymbol{v}^n,\boldsymbol{w}^n\boldsymbol{\phi}^n,\boldsymbol{\psi}^n,\boldsymbol{s}^n)$, $n=0,1$. Furthermore, we introduce the two diagonal matrices $\boldsymbol{L}=\{l_{ii}\}$ and $\boldsymbol{R}=\{r_{ii}\}$ via

$$l_{ii} = \frac{x_{i+1}^1 - x_i^0}{2} \quad \text{and} \quad r_{ii} = \frac{x_{i+1}^0 - x_i^1}{2}, \tag{35}$$

respectively. Hence the finite volume of the ith cell is given by

$$V_C = \Delta t(l_{ii} + r_{ii})$$

and we define the diagonal matrix

$$\boldsymbol{V}_C = \Delta t(\boldsymbol{L}+\boldsymbol{R}).$$

We also introduce midpoint values such as

$$\boldsymbol{u}^{1/2} = \frac{\boldsymbol{u}^1+\boldsymbol{u}^0}{2}$$

etc. Finally, we define spatially averaged values

$$\bar{\boldsymbol{v}}^n = \boldsymbol{A}\boldsymbol{v}^n,\ \bar{\boldsymbol{w}}^n = \boldsymbol{A}\boldsymbol{w}^n,\ \bar{\boldsymbol{u}}^n = \boldsymbol{A}\boldsymbol{u}^n,\ \bar{\boldsymbol{h}}^n = \boldsymbol{A}\boldsymbol{h}^n,\ \bar{\boldsymbol{s}}^n = \boldsymbol{A}\boldsymbol{s}^n,$$

$n = 0, 1/2, 1$. One time-step of the finite volume method can now be written as

$$\begin{aligned}
\boldsymbol{V}_C^{-1}\left[(\boldsymbol{L}+\boldsymbol{R}\boldsymbol{E})\boldsymbol{\psi}^1 - (\boldsymbol{L}\boldsymbol{E}+\boldsymbol{R})\boldsymbol{\psi}^0\right] &= \bar{\boldsymbol{v}}^{1/2} - 2\bar{\boldsymbol{u}}^{1/2} - 2\bar{\boldsymbol{u}}^{1/2}\cdot\bar{\boldsymbol{h}}^{1/2}, && (36)\\
\boldsymbol{V}_C^{-1}\left[(\boldsymbol{L}+\boldsymbol{R}\boldsymbol{E})(\boldsymbol{\phi}^1+2\alpha\boldsymbol{s}^1) - (\boldsymbol{L}\boldsymbol{E}+\boldsymbol{R})(\boldsymbol{\phi}^0+2\alpha\boldsymbol{s}^0)\right] &= \bar{\boldsymbol{w}}^{1/2} - \bar{\boldsymbol{u}}^{1/2}\cdot\bar{\boldsymbol{u}}^{1/2} - 2c_0^2\bar{\boldsymbol{h}}^{1/2}, && (37)\\
\Delta t\boldsymbol{D}\boldsymbol{v}^{1/2} + (\boldsymbol{L}+\boldsymbol{R}\boldsymbol{E})\boldsymbol{h}^1 - (\boldsymbol{L}\boldsymbol{E}+\boldsymbol{R})\boldsymbol{h}^0 &= \boldsymbol{0}, && (38)\\
\Delta t\boldsymbol{D}\boldsymbol{w}^{1/2} + (\boldsymbol{L}+\boldsymbol{R}\boldsymbol{E})\boldsymbol{u}^1 - (\boldsymbol{L}\boldsymbol{E}+\boldsymbol{R})\boldsymbol{u}^0 &= \boldsymbol{0}, && (39)\\
\Delta t\boldsymbol{V}_C^{-1}\boldsymbol{D}\boldsymbol{\psi}^{1/2} &= \bar{\boldsymbol{h}}^{1/2}, && (40)\\
\Delta t\boldsymbol{V}_C^{-1}\boldsymbol{D}\boldsymbol{\phi}^{1/2} &= \bar{\boldsymbol{u}}^{1/2}, && (41)\\
\alpha\boldsymbol{V}_C^{-1}\left[(\boldsymbol{L}+\boldsymbol{R}\boldsymbol{E})\boldsymbol{h}^1 - (\boldsymbol{L}\boldsymbol{E}+\boldsymbol{R})\boldsymbol{h}^0\right] &= \bar{\boldsymbol{s}}^{1/2}. && (42)
\end{aligned}$$

Here the dot product $\boldsymbol{a}\cdot\boldsymbol{b}$ of two vectors $\boldsymbol{a}$ and $\boldsymbol{b}$ is defined as the vector $\boldsymbol{c}$ with entries $c_i = a_i b_i$.

The scheme (36)-(42) is multi-symplectic when used with a parallelogram-like cell structure; i.e.

$$x_{i+1}^1 - x_i^0 = \Delta x + c\Delta t \quad \text{and} \quad x_{i+1}^0 - x_i^1 = \Delta x - c\Delta t,$$

which implies

$$(\boldsymbol{L}+\boldsymbol{R}\boldsymbol{E})\boldsymbol{h}^1 - (\boldsymbol{L}\boldsymbol{E}+\boldsymbol{R})\boldsymbol{h}^0 = \Delta x\boldsymbol{A}\left(\boldsymbol{h}^1-\boldsymbol{h}^0\right) - c\Delta t\boldsymbol{D}\boldsymbol{h}^{1/2}$$

etc., and

$$V_C = \Delta t\Delta x.$$

In fact, since $\boldsymbol{D}$ and $\boldsymbol{A}$ commute, one can now completely eliminate the variables $\boldsymbol{\psi}^n$ and $\boldsymbol{\phi}^n$, $n = 0, 1/2, 1$, by defining

$$\frac{1}{\Delta x}\boldsymbol{D}\boldsymbol{\psi}^n = \boldsymbol{A}\boldsymbol{h}^n \quad \text{and} \quad \frac{1}{\Delta x}\boldsymbol{D}\boldsymbol{\phi}^n = \boldsymbol{A}\boldsymbol{u}^n.$$

Thus we obtain the simplified system

$$\begin{aligned}
\boldsymbol{0} &= \bar{\boldsymbol{v}}^{1/2} - \bar{\boldsymbol{u}}^{1/2} - \bar{\boldsymbol{u}}^{1/2}\cdot\bar{\boldsymbol{h}}^{1/2},\\
\alpha\boldsymbol{V}_C^{-1}\left[(\boldsymbol{L}+\boldsymbol{R}\boldsymbol{E})\boldsymbol{s}^1 - (\boldsymbol{L}\boldsymbol{E}+\boldsymbol{R})\boldsymbol{s}^0\right] &= \bar{\boldsymbol{w}}^{1/2} - \frac{1}{2}\bar{\boldsymbol{u}}^{1/2}\cdot\bar{\boldsymbol{u}}^{1/2} - c_0^2\bar{\boldsymbol{h}}^{1/2},\\
\Delta t\boldsymbol{D}\boldsymbol{v}^{1/2} + (\boldsymbol{L}+\boldsymbol{R}\boldsymbol{E})\boldsymbol{h}^1 - (\boldsymbol{L}\boldsymbol{E}+\boldsymbol{R})\boldsymbol{h}^0 &= \boldsymbol{0},\\
\Delta t\boldsymbol{D}\boldsymbol{w}^{1/2} + (\boldsymbol{L}+\boldsymbol{R}\boldsymbol{E})\boldsymbol{u}^1 - (\boldsymbol{L}\boldsymbol{E}+\boldsymbol{R})\boldsymbol{u}^0 &= \boldsymbol{0},\\
\alpha\boldsymbol{V}_C^{-1}\left[(\boldsymbol{L}+\boldsymbol{R}\boldsymbol{E})\boldsymbol{h}^1 - (\boldsymbol{L}\boldsymbol{E}+\boldsymbol{R})\boldsymbol{h}^0\right] &= \bar{\boldsymbol{s}}^{1/2}.
\end{aligned}$$

Furthermore, since $\boldsymbol{A}$ commutes with $\boldsymbol{D}$, $\boldsymbol{L}+\boldsymbol{R}\boldsymbol{E}$, and $\boldsymbol{L}\boldsymbol{E}+\boldsymbol{R}$ on a parallelogram-like grid structure, one can reformulate the scheme in terms of its spatial midpoint values $\bar{\boldsymbol{v}}^n$, $\bar{\boldsymbol{w}}^n$, $\bar{\boldsymbol{u}}^n$, $\bar{\boldsymbol{h}}^n$, and $\bar{\boldsymbol{s}}^n$,

$n = 0, 1/2, 1$. This, finally, yields the scheme

$$
\begin{aligned}
\mathbf{0} &= \bar{\boldsymbol{v}}^{1/2} - \bar{\boldsymbol{u}}^{1/2} - \bar{\boldsymbol{u}}^{1/2} \cdot \bar{\boldsymbol{h}}^{1/2}, &(43)\\
\alpha \boldsymbol{V}_C^{-1} \left[(\boldsymbol{L} + \boldsymbol{R}\boldsymbol{E}) \boldsymbol{A}^{-1} \bar{\boldsymbol{s}}^1 - (\boldsymbol{L}\boldsymbol{E} + \boldsymbol{R}) \boldsymbol{A}^{-1} \bar{\boldsymbol{s}}^0 \right] &= \bar{\boldsymbol{w}}^{1/2} - \frac{1}{2} \bar{\boldsymbol{u}}^{1/2} \cdot \bar{\boldsymbol{u}}^{1/2} - c_0^2 \bar{\boldsymbol{h}}^{1/2}, &(44)\\
\Delta t \boldsymbol{D} \bar{\boldsymbol{v}}^{1/2} + (\boldsymbol{L} + \boldsymbol{R}\boldsymbol{E}) \bar{\boldsymbol{h}}^1 - (\boldsymbol{L}\boldsymbol{E} + \boldsymbol{R}) \bar{\boldsymbol{h}}^0 &= \mathbf{0}, &(45)\\
\Delta t \boldsymbol{D} \bar{\boldsymbol{w}}^{1/2} + (\boldsymbol{L} + \boldsymbol{R}\boldsymbol{E}) \bar{\boldsymbol{u}}^1 - (\boldsymbol{L}\boldsymbol{E} + \boldsymbol{R}) \bar{\boldsymbol{u}}^0 &= \mathbf{0}, &(46)\\
\alpha \boldsymbol{V}_C^{-1} \left[(\boldsymbol{L} + \boldsymbol{R}\boldsymbol{E}) \boldsymbol{A}^{-1} \bar{\boldsymbol{h}}^1 - (\boldsymbol{L}\boldsymbol{E} + \boldsymbol{R}) \boldsymbol{A}^{-1} \bar{\boldsymbol{h}}^0 \right] &= \bar{\boldsymbol{s}}^{1/2}. &(47)
\end{aligned}
$$

This scheme provides a compact discretization of the dispersive shallow-water system (13)-(14) which is, in principle, applicable to arbitrary cell geometries and is equivalent to the multi-symplectic scheme (36)-(42) for parallelogram-like cells. Note that the scheme could be compactified even further by also eliminating the variables $\bar{\boldsymbol{v}}^{1/2}$ and $\bar{\boldsymbol{w}}^{1/2}$.

We assume that the associated discretization of the linearized shallow-water equations (17); i.e.,

$$
\begin{aligned}
\mathbf{0} &= \bar{\boldsymbol{v}}^{1/2} - \bar{\boldsymbol{u}}^{1/2},\\
\alpha \boldsymbol{V}_C^{-1} \left[(\boldsymbol{L} + \boldsymbol{R}\boldsymbol{E}) \boldsymbol{A}^{-1} \bar{\boldsymbol{s}}^1 - (\boldsymbol{L}\boldsymbol{E} + \boldsymbol{R}) \boldsymbol{A}^{-1} \bar{\boldsymbol{s}}^0 \right] &= \bar{\boldsymbol{w}}^{1/2} - c_0^2 \bar{\boldsymbol{h}}^{1/2},\\
\Delta t \boldsymbol{D} \bar{\boldsymbol{v}}^{1/2} + (\boldsymbol{L} + \boldsymbol{R}\boldsymbol{E}) \bar{\boldsymbol{h}}^1 - (\boldsymbol{L}\boldsymbol{E} + \boldsymbol{R}) \bar{\boldsymbol{h}}^0 &= \mathbf{0},\\
\Delta t \boldsymbol{D} \bar{\boldsymbol{w}}^{1/2} + (\boldsymbol{L} + \boldsymbol{R}\boldsymbol{E}) \bar{\boldsymbol{u}}^1 - (\boldsymbol{L}\boldsymbol{E} + \boldsymbol{R}) \bar{\boldsymbol{u}}^0 &= \mathbf{0},\\
\alpha \boldsymbol{V}_C^{-1} \left[(\boldsymbol{L} + \boldsymbol{R}\boldsymbol{E}) \boldsymbol{A}^{-1} \bar{\boldsymbol{h}}^1 - (\boldsymbol{L}\boldsymbol{E} + \boldsymbol{R}) \boldsymbol{A}^{-1} \bar{\boldsymbol{h}}^0 \right] &= \bar{\boldsymbol{s}}^{1/2},
\end{aligned}
$$

is solvable. In other words, the matrix

$$
\begin{bmatrix}
-\frac{1}{2}\boldsymbol{I} & \mathbf{0} & \frac{1}{2}\boldsymbol{I} & \mathbf{0} & \mathbf{0}\\
\mathbf{0} & \frac{c_o^2}{2}\boldsymbol{I} & \mathbf{0} & -\frac{1}{2}\boldsymbol{I} & \alpha\boldsymbol{C}\\
\mathbf{0} & \boldsymbol{B} & \frac{\Delta t}{2}\boldsymbol{D} & \mathbf{0} & \mathbf{0}\\
\boldsymbol{B} & \mathbf{0} & \mathbf{0} & \frac{\Delta t}{2}\boldsymbol{D} & \mathbf{0}\\
\mathbf{0} & \alpha\boldsymbol{C} & \mathbf{0} & \mathbf{0} & -\frac{1}{2}\boldsymbol{I}
\end{bmatrix},
$$

with

$$
\boldsymbol{B} = \boldsymbol{L} + \boldsymbol{R}\boldsymbol{E} \quad \text{and} \quad \boldsymbol{C} = \boldsymbol{V}_C^{-1} \boldsymbol{B} \boldsymbol{A}^{-1},
$$

is invertible. Then the equations (43)-(47) can be solved for the "unknowns" $(\bar{\boldsymbol{u}}^1, \bar{\boldsymbol{h}}^1, \bar{\boldsymbol{v}}^1, \bar{\boldsymbol{w}}^1, \bar{\boldsymbol{s}}^1)$ provided Δt is sufficiently small.

6 Time-Dependent Problems and Reversible Moving Mesh Methods

We now focus on time-dependent problems of type (23) and its discretization by the finite volume method (25). Let us assume that a step-size Δt has been chosen and is kept constant during the interval of integration. Thus we only consider time integration from $t_0 = 0$ to $t_1 = \Delta t$. We assume now that a spatial grid is given at time $t_0 = 0$. We denote this grid by $\{x_i^0\}$, $i = 1, \ldots, M$, M the number of grid points. The next step is to chose a spatial grid $\{x_i^1\}$, $i = 1, \ldots, M$, at time $t_1 = \Delta t$. This leads to the discrete formulation

$$
\begin{aligned}
&\frac{1}{V_C} \mathbf{K} \left(\frac{\boldsymbol{z}_{i+1}^1 + \boldsymbol{z}_{i+1}^0}{2} \Delta t - \frac{\boldsymbol{z}_i^1 + \boldsymbol{z}_i^0}{2} \Delta t \right) + \\
&\frac{1}{V_C} \mathbf{L} \left(\frac{\boldsymbol{z}_i^1 - \boldsymbol{z}_{i+1}^0}{2} (x_{i+1}^1 - x_i^0) + \frac{\boldsymbol{z}_{i+1}^1 - \boldsymbol{z}_i^0}{2} (x_{i+1}^0 - x_i^1) \right) = \boldsymbol{\nabla}_{\boldsymbol{z}} S(\boldsymbol{z}_c)\,, \qquad (48)
\end{aligned}
$$

where

$$V_C = \Delta t \frac{x_{i+1}^1 + x_{i+1}^0 - x_i^1 - x_i^0}{2}.$$

If the new mesh satisfies $x_i^1 = x_i^0$ for all $i = 1, \ldots, M$, then the mesh is said to be *constant* and the method (48) reduces to the well-known Preissman box scheme. On the other hand, if there is a constant c such that $x_i^1 = x_i^0 + c\Delta t$ for all $i = 1, \ldots, M$, then we obtain a particular example of a *moving mesh method* which also satisfies the conditions (29)-(30). It can be understood as a box scheme discretization of the "moving frame" PDE (32).

A general moving mesh $x_i^1 = x_i^0 + c_i \Delta t$, $i = 1, \ldots, M$, $\{c_i\}$ appropriate constants, will lead to a finite volume discretization that is *not* multi-symplectic. Nevertheless such schemes are potentially very useful since they allow for a mesh adaption as it might be necessary to resolve less smooth solution components. Various possibilities to adjust the mesh seem feasible [10, 5]. We only like to mention two. (i) The grid is determined at each time-level as the solution of a system of algebraic equations

$$d_j(\{\boldsymbol{z}_i^1\}, \{x_i^1\}, t_0) = 0, \qquad (j = 1, \ldots, M).$$

Often the functions $\{d_j\}$ are determined using the principle of mesh equidistribution [10] and/or invariance under symmetries [5]. (ii) We formulate a system of differential equations

$$\frac{d}{dt} x_i = f(\boldsymbol{z}(x_i)), \qquad (i = 1, \ldots, M), \tag{49}$$

which is discretized in time using

$$x_i^1 = x_i^0 + \Delta t f\left(\frac{\boldsymbol{z}_i^1 + \boldsymbol{z}_i^0}{2}\right). \tag{50}$$

A differential equation of type (49) can be obtained by rephrasing the approach (i) in a dynamical framework [10, 12], by using characteristic directions [9], or by applying a semi-Lagrangian formalism based on symmetry considerations [6, 5]. In §7, we apply approach (ii) to the dispersive shallow-water system.

Similar to time-reversible ODEs (see, for example, [17]), it might be advantageous to adjust the mesh in a reversible manner such as to obtain a *reversible discretization*. For that reason, let us assume that the given multi-symplectic PDE satisfies a reversing symmetry $(\mathbf{R}, \mathbf{J})$. We also assume that the differential equation (49) is chosen so that it satisfies the same reversing symmetry. Then the corresponding moving mesh discretization (48) and (50) is called *reversible*, if it is invariant under the reversing symmetry $(\mathbf{R}, \mathbf{J})$; i.e., if $\{\boldsymbol{z}_i^n\}$, $n = 0, 1$, satisfies (48), then $\{\mathbf{R}\boldsymbol{z}_i^n\}$, $n = 0, 1$, satisfies (48) and (50) with Δt and $\{x_i^n\}$ replaced by $\Delta \bar{t}$ and $\{\bar{x}_i^n\}$, where $(\Delta \bar{t}, \bar{x}_i^n)^T = \mathbf{J}(\Delta t, x_i^n)^T$. We stress that this definition requires the method to be *symmetric* in space and time. To be more specific, given a mesh $\{x_i^0\}$ and solutions $\{\boldsymbol{z}_i^0\}$, we integrate one step forward in time and obtain the mesh $\{x_i^1\}$ and solutions $\{\boldsymbol{z}_i^1\}$. Now we reverse time and integrate one step backward in time using the mesh $\{x_i^1\}$ and the solutions $\{\boldsymbol{z}_i^1\}$. Then we say that the mesh is adjusted in a *time symmetric* manner, if this leads us back to the mesh $\{x_i^0\}$ and the solutions $\{\boldsymbol{z}_i^0\}$. The spatial symmetry of a method is defined in a similar manner; i.e., exchanging the indices i and $i+1$ in (48) should lead back to (48). It is easily checked that (48) together with (50) is indeed symmetric in space and time and, therefore, reversible if used with a proper function f in (50).

The PDE (23) possesses an energy and a momentum conservation law. The associated volume integrals are approximated by

$$\begin{aligned}\Big(S(\boldsymbol{z}_{i+1/2}^0)(x_1^0 - x_0^0) + S(\boldsymbol{z}_{i+1}^{1/2})(x_1^1 - x_1^0) + S(\boldsymbol{z}_{i+1/2}^1)(x_0^1 - x_1^1) + S(\boldsymbol{z}_i^{1/2})(x_0^0 - x_0^1)\Big)& \\ - \ \big(\langle \boldsymbol{z}_i^0, \mathbf{L}\boldsymbol{z}_{i+1}^0\rangle + \langle \boldsymbol{z}_{i+1}^0, \mathbf{L}\boldsymbol{z}_{i+1}^1\rangle + \langle \boldsymbol{z}_{i+1}^1, \mathbf{L}\boldsymbol{z}_i^1\rangle + \langle \boldsymbol{z}_i^1, \mathbf{L}\boldsymbol{z}_i^0\rangle\big) \ &= \ \delta E_{i+1/2}^{1/2}\end{aligned} \tag{51}$$

in case of the energy conservation law (ECL), and by

$$\Delta t\left(S(\boldsymbol{z}_{i+1}^{1/2})-S(\boldsymbol{z}_i^{1/2})\right)-\left(\langle \boldsymbol{z}_i^0,\mathbf{K}\boldsymbol{z}_{i+1}^0\rangle+\langle \boldsymbol{z}_{i+1}^0,\mathbf{K}\boldsymbol{z}_{i+1}^1\rangle+\langle \boldsymbol{z}_{i+1}^1,\mathbf{K}\boldsymbol{z}_i^1\rangle+\langle \boldsymbol{z}_i^1,\mathbf{K}\boldsymbol{z}_i^0\rangle\right)=\delta M_{i+1/2}^{1/2}$$

in case of the momentum conservation law. The residuals $\{\delta E_{i+1/2}^{n+1/2}\}$ and $\{\delta M_{i+1/2}^{n+1/2}\}$ are non-zero, in general. The magnitude of the residuals provides a good numerical test for the accuracy of the computed solutions.

7 Numerical Experiments

7.1 Linear Wave Equation

We implement a finite volume method for the linear shallow-water equations (15) as outlined in §5. We use periodic boundary conditions $u(x,t)=u(x+L,t)$ etc., $L=10$, and initial conditions

$$h(x,0)=0.3\left(\mathrm{e}^{-(x-L/2)^2}-\sqrt{\pi}\right)+1, \qquad u(x,h)=0. \tag{52}$$

For $\alpha=0$, the exact solution has a particularly simple form. The initial shape splits into two bumps of a lower amplitude moving at a wave spead $\pm c_o$, $c_o=1$. At the boundaries the waves then reflect back so $u(x,10)=u(x,0)$. Note that (17) with $\alpha=0$ is equivalent to the linear wave equation

$$u_t+c_o^2h_x=0, \qquad h_t+u_x=0,$$

and note that the discretization (43)-(47) reduces to a standard cell-vertex finite volume discretization of this system of conservation laws.

Since the solution of the linearized system (17) with $\alpha=0$ is periodic with period $T=10$, we integrate over a time interval $[0,T]$ using N steps of step-size $\Delta t=T/N$. The spatial mesh is kept fixed with mesh-size $\Delta x=k\cdot\Delta t$, $k=1/2,1,2$. We first observe that the discrete energy conservation law is exactly satisfied. Next we compute the global solution error

$$\delta h_{max}:=||\boldsymbol{h}(t=T)-\boldsymbol{h}(t=0)||_\infty$$

at $T=10$. See Tab. 7.1. Note the exeptionally high accuracy of the solution for $k=1$; i.e. $\Delta t=\Delta x$.

global error	$\Delta t=0.25$	$\Delta t=0.125$	$\Delta t=0.0625$
$k=2$	0.0678	0.0190	0.0018
$k=1$	1.1e-04	1.9e-06	3.0e-08
$k=1/2$	0.0159	0.0015	0.0001

Table 1: Global error δh_{max} for the linear wave equation. The spatial mesh is held fixed with a mesh-size $\Delta x=k\cdot\Delta t$.

We also implement a moving mesh approach with

$$\frac{d}{dt}x=1$$

using the same parameter set as described above. See Tabs. 7.1 for the numerical results.

Finally, we integrate (17), $\alpha=0$, over several periods of length $T=10$ and compute

$$\delta h_{max}^k=||\boldsymbol{h}(kT)-\boldsymbol{h}(0)||_\infty, \qquad k=1,2,\ldots,$$

for $\Delta t=0.0625$ and $\Delta x=0.125$, $\Delta t=0.0625$ and $\Delta x=0.0625$, as well as $\Delta t=0.125$ and $\Delta x=0.0625$ using a fixed mesh. The results can be found in Fig. 3.

global error	$\Delta t = 0.25$	$\Delta t = 0.125$	$\Delta t = 0.0625$
$k = 2$	0.0247	0.0031	0.0004
$k = 1$	0.0739	0.0389	0.0117
$k = 1/2$	0.0774	0.0457	0.0146

Table 2: Global error δh_{max} for the linear wave equation. The spatial mesh is moved with a constant speed $c = 1$ and the mesh-size is $\Delta x = k \cdot \Delta t$.

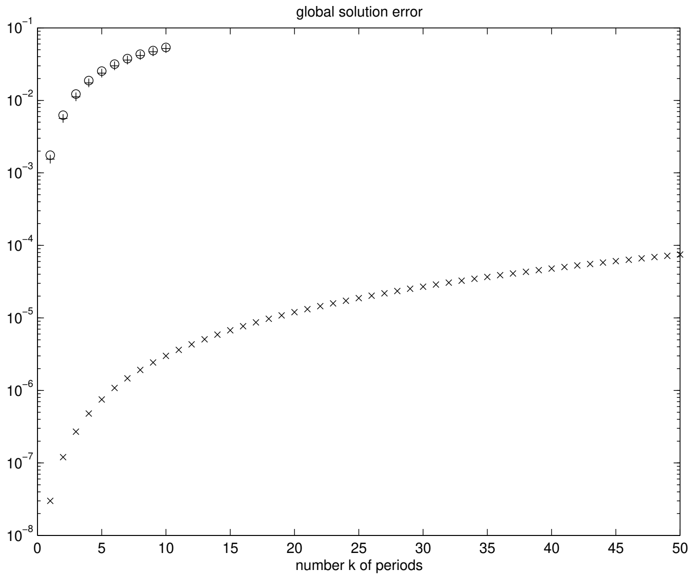

Figure 3: Global error δh_{max}^k, $k \geq 1$, for the linear wave equation with $\Delta t = 0.0625$ and $\Delta x = 0.125$ (o), $\Delta t = 0.0625$ and $\Delta x = 0.0625$ (x), and $\Delta t = 0.125$ and $\Delta x = 0.0625$ (+).

7.2 Nonlinear Shallow-Water Equations

We now consider the dispersive nonlinear shallow-water equations (15) with initial conditions

$$h(x,0) = 0.3\left(\mathrm{e}^{-(x-L/2)^2} - \sqrt{\pi}\right) + 1, \qquad u(x,h) = 2\sqrt{h(x,0)} - 2. \tag{53}$$

For $\alpha = 0$, these initial conditions lead to a wave traveling along characteristics given by

$$\frac{d}{dt}x = 3\sqrt{h} - 2. \tag{54}$$

Hence the initial data (53) develops into a shock. This non-smooth solution behavior can be avoided by using $\alpha = \Delta x$ which replaces the shock by a moving oscillatory front. The steepness of the front and the width of the oscillations depends on the size of the parameter α. See Figs. 4 and 5 for numerical results using a fixed mesh. The residuals $\{\delta E_{i+1/2}^{n+1/2}\}$ in the discrete energy conservation law (ECL) are defined by (51). We also introduce the maximum error in the ECL per time step by

$$\delta E_{max}^{n+1/2} = \max_i |\delta E_{i+1/2}^{n+1/2}|.$$

Finally, we compute the solution of the regular shallow-water system ($\alpha = 0$) with initial condition (53). To be able to resolve the formation of the shock at $t \approx 2.75$, we use a moving mesh based on the differential equation (54). In Fig. 6, we plot the layer depth at $t = 2.75$, the residual in the

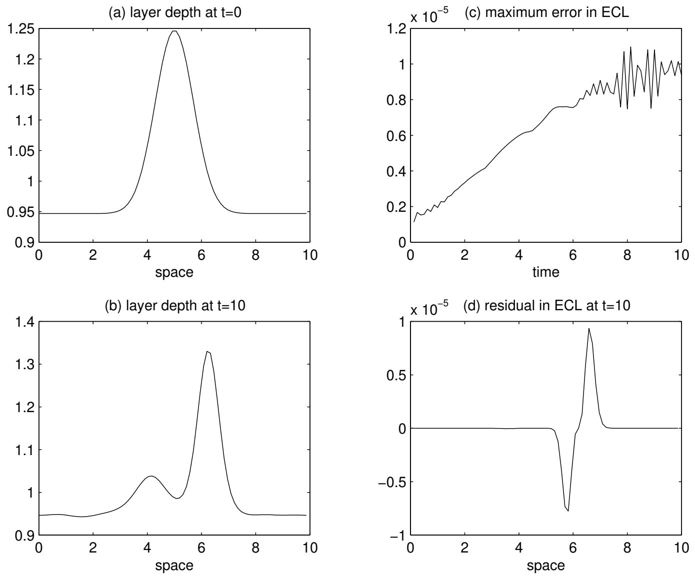

Figure 4: Numerical results for the dispersive shallow-water equations (15) with $\alpha = \Delta x$, $\Delta x = 0.125$, and $\Delta t = 0.125$.

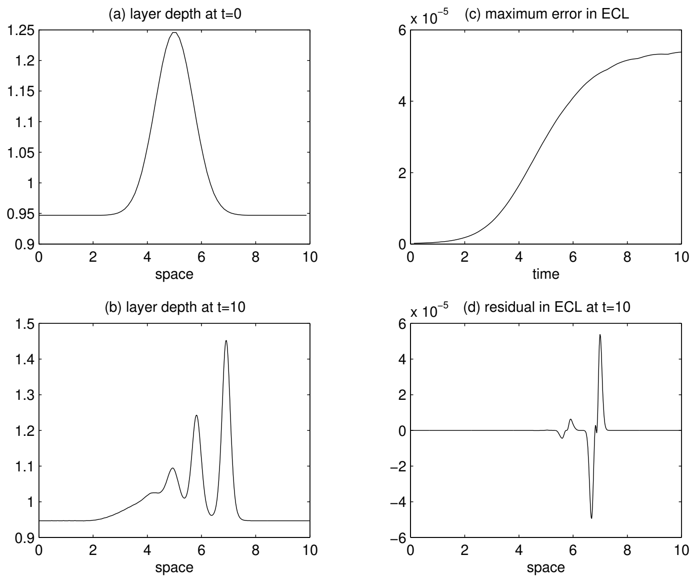

Figure 5: Numerical results for the dispersive shallow-water equations (15) with $\alpha = \Delta x$, $\Delta x = 0.015$, and $\Delta t = 0.125$.

ECL at $t = 2.75$, the maximum error in the ECL as a function of time, and the position of the grid points $\{x_i\}$ at time $t = 2.75$. Note that, at $t = 2.75$, more mesh points have been moved into the region of shock formation near $x \approx 9$. See Fig. 6(b).

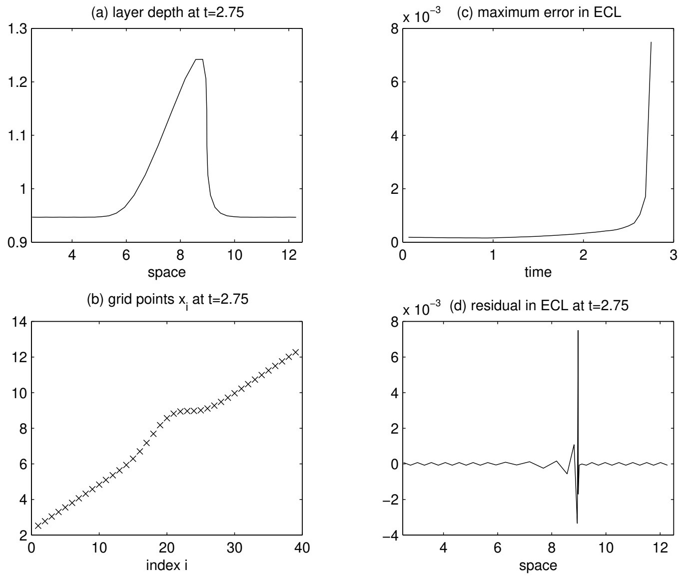

Figure 6: Numerical results for the regular shallow-water equations (15) with $\Delta x = 0.25$, and $\Delta t = 0.0625$.

8 Conclusion

We have used the general framework of multi-symplecticity to discuss cell-vertex finite volume methods in the context of conservative (Hamiltonian) PDEs. Conditions on the discretization and the shape of the finite volume cells have been formulated that insure the existence of a discrete conservation law of symplecticity. This discrete conservation law can be viewed as a proper generalization of the concept of symplectic discretizations for Hamiltonian ODEs [4].

Although the methods considered in this paper are implicit, consideration of specific Hamiltonian PDEs can be expected to lead to more efficient multi-symplectic finite volume schemes.

We introduced the concept of reversible methods and applied it to a system of conservation laws using the general formulation (48) as a starting point. Note that non of the (non-constant) moving mesh methods presented here can be expected to be multi-symplectic. In this respect the situation appears to be similar to that for Hamiltonian ODEs and variable step-size methods [17].

References

[1] M. B. Abbott & D. R. Basco, *Computational Fluid Dynamics*, Longman Scientific & Technical, 1989.

[2] T. J. Bridges, *Multi-symplectic structures and wave propagation*, Math. Proc. Camb. Phil. Soc. **121** (1997) 147–190.

[3] Th. J. Bridges, *A geometric formulation of the conservation of wave action and its implications for signature and the classification of instabilities*, Proc. R. Soc. Lond. A **453** (1997), 1365–1395.

[4] Th. J. Bridges & S. Reich, *Multi-symplectic integrators: numerical schemes for Hamiltonian PDEs that conserve symplecticity*, technical report.

[5] C. J. Budd & G. J. Collins, *Symmetry based numerical methods for partial differential equations*, Proc. 1997 Dundee Conference in Numerical Analysis, (1997), 16–36.

[6] V. Dorodnitsyn, *Continuous Symmetries of Finite-Difference Evolution Equations and Grids*, Centre de Recherches Mathématiques, CRM Proceedings and Lecture Notes Vol. 9 (1996), 103–112.

[7] D. R. Durrand, *Numerical Methods for Wave Equations in Geophysical Fluid Dynamics*, Springer-Verlag, New York, 1999.

[8] J. H. Ferziger & M. Perić, *Computational Methods for Fluid Dynamics*, Springer-Verlag, Berlin, 1996.

[9] A. Harten & J. M. Hyman, *A self-adjusting grid for the computation of weak solutions of hyperbolic conservation laws*, J. Comput. Phys. **50** (1983), 235–269.

[10] W. Huang, Y. Ren & R. D. Russell, *Moving mesh methods based on moving mesh partial differential equations.*, J. Comput. Phys. **112** (1994), 279–290.

[11] P. James & R. Bonnerot, *Numerical solution of the Eulerian equations of compressible flow by a finite volume method which follows the free boundary and the interface*, J. Comput. Phys. **18** (1975), 21–45.

[12] S. Li & L. Petzold, *Moving mesh methods with upwinding schemes for time-dependent PDEs*, J. Comput. Phys. **131** (1997), 368–377.

[13] J. E. Marsden, G. P. Patrick & S. Shkoller, *Multisymplectic geometry, variational integrators, and nonlinear PDEs*, Comm. in Math. Phys. **199** (1999), 351–395.

[14] K. W. Morton, M. Stynes & E. Süli, *Analysis of a cell-vertex finite volume method for convection-diffusion problems*, Mathematics of Computation **66**, 1389–1406, 1997.

[15] K. W. Morton & E. Süli, *Finite volume methods and their analysis*, IMA J. Num. Anal. **11** (1991), 241–260.

[16] S. Reich, *Multi-symplectic Runge-Kutta collocation methods for Hamiltonian wave equations*, J. Comput. Phys. **157** (2000), 473–499.

[17] D. Stoffer, *Variable steps for reversible methods*, Computing **55** (1995), 1–22.

[18] E. Süli, *The accuracy of cell-vertex finite volume methods on quadrilateral meshes*, Math. Comput **59** (1992), 359–382.

[19] G. W. Whitham, *Linear and Nonlinear Waves*, John Wiley & Sons, 1974.